Asian Journal of Chemistry Vol. 20, No. 3 (2008), 2275-2282

Long-Range Heterogeneous Electron Transfer of Ferrocene Functionalized Gold Nanoparticles Through Alkanethiol Bridges at Gold Electrodes

JIONG ZHANG‡, LIHUA WANG†, YING WAN†, XIAOLEI ZUO†,
SHIPING SONG*†, ZHIZHOU ZHANG*†† and CHUNHAI FAN†
†*Shanghai Institute of Applied Physics, Chinese Academy of Sciences*
Shanghai-201800, P.R. China
Fax: (86)(21)59556902; E-mail: spsong@sinap.ac.cn; zhangzz@tust.edu.cn

The heterogeneous electron-transfer rate constants between gold electrodes and ferrocene either attached to the electrode surface directly by an alkanethiol bridge or anchored to gold nanoparticles which adsorbed on the electrode were measured using cyclic voltammetry. For the ferrocene directly attached to the electrode through an undecanethiol linkage we found the different density of redox molecules exhibited different electron-transfer rate constants. In this work, the ferrocene anchoring to gold nanoparticles (AuNPs) led to very stable functionalized nanoparticles, which possessed well electrochemical activity.

Key Words: Electron-transfer rate constants, Ferrocene, Gold nanoparticles.

INTRODUCTION

A promising approach for the development of electrochemical biosensors is to establish a direct electrical communication between the biomolecules and the electrode surface. Long-range bridge-mediated electron transfer is a critical element of the mechanisms of action of many biological superstructures and the developing field of molecular electronics[1].

Bridge-mediated electron transfer of ferrocene groups on electrodes has been the subject of extensive study for many years[2-13]. In general it is the case that the electron-transfer rate constant is controlled by the organized structure of the packing SAM, the orientation of the ferrocene in the layers and distance (bridge length) between the redox and the electrode[14]. In the present work we showed the assembled-density of ferrocene groups in the monolayer affected the electron transfer rate constant between

‡Graduate School of the Chinese Academy of Sciences, Beijing-100039, P.R. China.
††Tianjin University of Science and Technology, Tianjin-300040, P.R. China, E-mail: zhangzz@tust.edu.cn

ferrocene and gold electrodes. The different density of ferrocenylthiol SAM was obtained from incubating the electrodes in ferrocenylthiol solutions of different concentrations.

Metal and semiconductor nanoparticles exhibit unique properties because of their nano-scale and high proportion of surface atoms, which are significantly different from those of the corresponding bulk materials[15]. The great application potential of these nanoparticles or redox functionalized ones as building blocks for the construction of electronic nano-materials, such as single electron devices and sensitive electrometers, had drawn much attention[9,16-19]. The ferrocene molecule has extensive applications in electrochemical biosensors because of its excellent electrochemical activities. In this study, the ferrocene functionalized gold nanoparticles optically and electrochemically are synthesized and characterized. It was found that the ferrocene-functionalized AuNPs possessed well electrochemical stability and activity. They may also be proposed for the potential application of bio-electrochemical devices[20] and electrochemical biosensors in future.

EXPERIMENTAL

11-Ferrocenyl-1-undecanethiol (FUT) was from Prochimia. Gold nanoparticles (AuNPs, 20 ± 3 nm, *ca.* 0.01 % $HAuCl_4$), mercaptohexanol (MCH), sodium perchlorate ($NaClO_4$), N,N-dimethylformamide (DMF) and 11-mercapto-1-undecanol (MCU) were from Sigma. Buffers for both electrochemistry and electrode washing are 1 M $NaClO_4$ solutions. All solutions were prepared with Milli-Q water (18 MΩ·cm resistivity) from a Millipore system.

Preparation of ferrocenyl-undecanethiol-capped gold nanoparticle conjugates: Conjugates of fc-capped-AuNPs were synthesized as follows: The gold nanoparticle solution was mixed with DMF containing ferrocenyl-undecanethiol with a final concentration of 250 μM on a stirrer at 800 rpm for 24 h. The solution was then centrifuged at 12000 rpm for 20 min and the excess reagents containing ferrocenyl-undecanethiol was decanted. The red oily precipitate was thoroughly rinsed, recentrifuged and then dispersed in water solution.

Ferrocenyl-undecanethiol and ferrocene-capped-AuNPs modified gold electrodes: Gold electrodes (2 mm in diameter, CH Instruments Inc., Austin) were first polished on microcloth (Buehler) with Gamma micropolish deagglomerated alumina suspension (0.05 μm) for 5 min. Residual alumina powder were removed by sonicating electrodes in ethanol and water for 5 min, respectively. Then the electrodes were electrochemically cleaned to remove any remaining impurities[21]. After being dried with nitrogen, electrodes were immediately used for mercapto-self-assembling.

Electrodes modified with ferrocenylundecanethiol-mercaptohexanol (FUT-MCH) and ferrocenylundecanethiol-mercaptoundecanol (FUT-MCU) mixed self-assembly monolayers were investigated in this work. FUT surfaces were obtained by incubation of electrodes with 1, 2 or 5 mM of FUT for 1 h. The FUT modified electrodes were further treated with 2 mM MCH for 4 h or with 2 mM MCU for 4 h in order to obtain well-aligned monolayers. To attach the Fc-capped gold nanoparticle conjugates onto the electrode surface covered with a given SAM, the electrode prepared with aforementioned cleaning procedure was first allowed for react with 2 mM MCH for 4 h or with 2 mM MCU for 4 h. Subsequently, the electrodes were exposed to the Fc-capped gold nanoparticle conjugate solution for 1 h at room temperature. Finally, after rinsed with water, the electrode was transferred to a 1 M $NaClO_4$ solution and characterized voltammetrically.

Electrochemical measurements: All electrochemical measurements were performed with a CHI 430 electrochemical workstation (CH Instruments Inc., Austin). A conventional three-electrode configuration was employed all through the experiment, which involved a gold working electrode, a platinum wire auxiliary electrode and an Ag/AgCl (3 M KCl) reference electrode. Supporting electrolyte is 1 M $NaClO_4$. Cyclic voltammetry (CV) was carried out in a scan-rate range from 20 to 1000 V/s.

RESULTS AND DISCUSSION

Electrochemical characterization of FUT-MCH modified electrode: First, we investigated the electrochemical properties of the gold electrode modified with FUT-MCH SAM. Fig. 1 showed the cyclic voltammetric features of the surface-bound FUT molecules. The anodic and cathodic current peaks are symmetrically shaped and the peak currents linearly increase over the range of scan rates from 0.05 to 2.00 V/s, the linear regression equation $I_p = 1.1645 + 10.2802v$ ($R = 0.9990$). The peak separation (ΔEp) between the cathodic and anodic peaks is 11 mV and the full width at half-maximum is *ca.* 85 mV at a scan rate of 100 mV/s, which is close to the theoretical for a reversible 1e electrode process. Significant alterations in the shape of the cyclic voltammogram curves are observed and the peak currents linearly increase with square root of scan rate at higher scan rates for values from 5 to 200 V/s, the equation $I_p = -44.6179 + 39.2087v^{1/2}$ ($R = 0.9989$). These results indicated that the redox reaction happened on the electrode was controlled by surface-confined at a lower scan rate and was controlled by diffusion at a scan rate higher than 2 V/s. From the cyclic voltammogram, the surface coverage of FUT was calculated by the equation[22] assuming that all of the ferrocene sites are electrochemically active. Using this approach, the calculated value of Γ_{Fc} is 3.51×10^{-10} mol/cm^2.

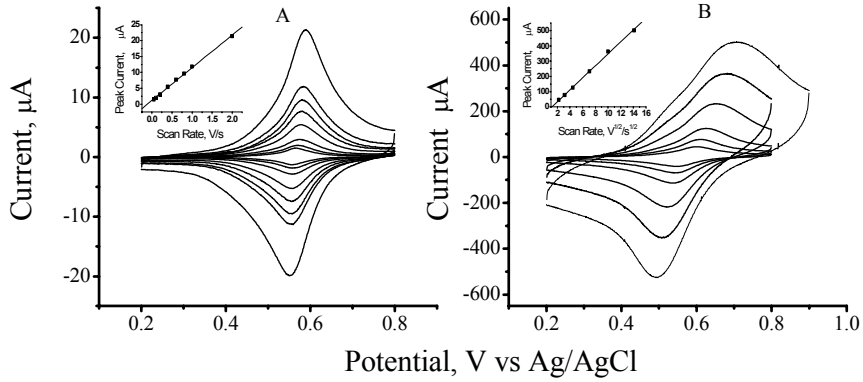

Fig. 1. Cyclic voltammograms of ferrocenyl-undecanethiol and mercaptohexanol mixed monolayer containing 3.51×10^{-10} mol/cm^2 of ferrocene sites. Supporting electrolyte is 1 M $NaClO_4$. (A) Scan rate = 0.05, 0.10, 0.20, 0.40, 0.60, 0.80, 1.00 and 2.00 V/s. Inset is plot of the oxidation peak current as a function of the scan rate. (B) Scan rate = 5, 10, 20, 50, 100 and 200 V/s. Inset is plot of the oxidation peak current as a function of the square root of the scan rate

Spectroscopic characterization of FUT functionalized gold nanoparticles: The self-assembling of ferrocenylthiol on AuNPs is similar to the thiolated single-strands DNA functionalizing nanoparticles. Both of them are attractive options for biosensing and future nanotechnological developments.

We prepared the ferrocene-functionalized gold nanoparticles by ferrocenyl-undecanethiol self-assembling on the gold nanoparticles of 20 nm in diameter. UV spectroscopy was employed to determine the character of fc-functionalized gold nanoparticles. As shown in Fig. 2, the peak at 280 nm is the characteristic absorption of ferrocene in 5 μM concentration (dotted line) and the absorbability at 525 nm (solid line) represents gold nanoparticles in 20 nm diameter. As to the ferrocenyl-functionalized nanoparticles, two absorption peaks at 270 nm and 525 nm were observed simultaneously. This feature clearly demonstrates the presence of ferrocenyl groups on the nanoparticles.

Electrochemical study of FUT functionalized AuNPs modified electrode: Fc-AuNPs-MCH and Fc-AuNPs-MCU were constructed by adsorbing the FUT functionalized gold nanoparticles to MCH and MCU self-assembled gold electrode surface, respectively. The structures of the two kinds of Fc-AuNPs modified electrodes were same except the different distances between Fc-AuNPs and electrodes caused by different chain-length of mercaptoanol.

The typical cyclic voltammograms after scanning repeatedly of two kinds of ferrocenyl-modified gold electrodes were observed in Fig. 3. The adsorption of FUT functionalized gold nanoparticles was observed on the

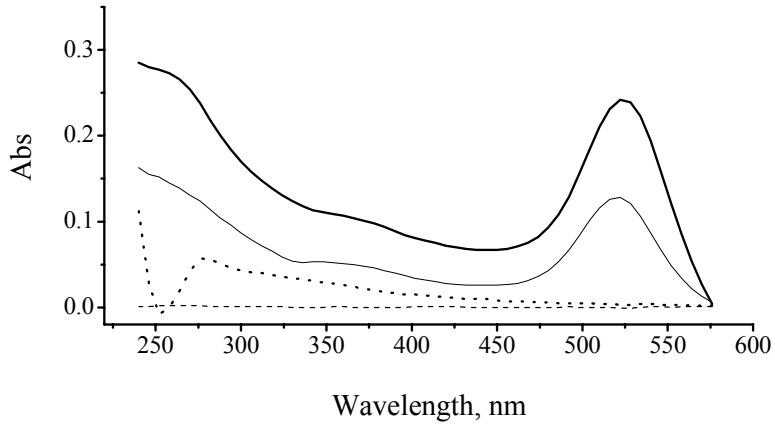

Fig. 2. UV absorption curves of 5 μM ferrocenyl-undecanethiol (dotted line), 1 nM gold nanoparticles (solid line) and 1 nM ferrocene-functionalized AuNPs (thick line)

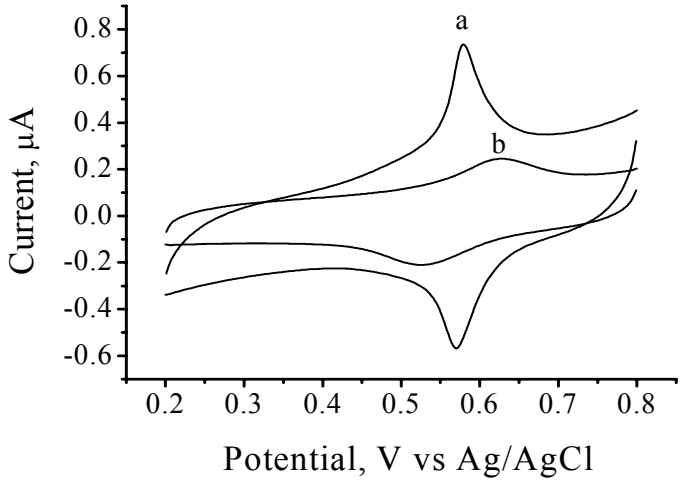

Fig. 3. Cyclic voltammograms of the fc-capped-AuNPs-modified gold electrodes assembled with MCH (a) and MCU (b), respectively. Supporting electrolyte: 1 M $NaClO_4$, scan rate: 0.1 V/s

alkanethiol-assembled gold electrode surface. The oxidation peaks at 578 mV for Fc-AuNPs-MCH and 632 mV for Fc-AuNPs-MCU and the ratio of I_{pa} to I_{pc} showed that the ferrocenyl groups are robustly attached to the gold nanoparticles which adsorbed on the electrode and the Fc-AuNPs possessed well electrochemical activities within the experimental potential range. Fc-AuNPs-MCH showed reversible redox behaviour at this scan rate because the peak-to-peak distance was less than 20 mV. As to Fc-AuNPs-MCU, ferrocenyl-functionalized nanoparticles adsorbed on MCU, oxidation

and reduction peaks were well-separated (*ca.* 100 mV). The appearance of the oxidation peak at a higher potential and the reduction peak at a lower one compared to Fc-AuNPs-MCH indicated that the current responded more sluggishly to the applied voltage. It is well-known that the electron-transfer rate constant is critically distance dependent while the other circumstances are same[14]. This indicated clearly the electron transfer process of Fc-AuNPs-MCU was slower than that of Fc-AuNPs-MCH because of the longer length of alkyl chain. Under the range of scan rate 0.05-2.00 V/s, the oxidation peak currents of ferrocene in Fc-AuNPs-MCH lightly linearly increase with the square root of scan rate (data not shown). The result manifested the redox showed a 'mixed' diffusion-adsorption behaviour.

Electron-transfer kinetics of FUT and FUT function-alized AuNPs modified electrode: Electron transfer rates between ferrocene and electrode were measured for two series of ferrocene-based monolayers. One was the ferrocene molecule linked to the gold electrode immediately by an alkane chain and another was the ferrocene group modified gold nanoparticles which adsorbed on the alkanethiolate self-assembled electrode. Both series of SAMs were studied using cyclic voltammetry method to measure the standard electron-transfer rate constants of the ferrocene groups. Theory enabling measurement of heterogeneous electron transfer rates from cyclic voltammetric oxidation-reduction peak potential separations, E_{peak}, was presented by Nicholson and Shain[23] for diffusing and by Laviron[24] for diffusionless electrochemical systems. This methodology is appealing by its ease of application; standard electron-transfer rate constants (k^0) result from analysis of the dependence of E_{peak} values on potential sweep rate using numerically generated working curves or explicit expressions[24]. The electron-transfer rate constants of all kinds of FUT-modified electrodes were determined by plotting the E_{peak} over potentials ($E_{peak} - E_{0'} = 0.5\Delta E_{peak}$) *vs.* log ($v/k_0$) based on heterogeneous Marcus kinetics[23]. The distance between the simulation of the overpotentials *vs.* log (v/k_0) and the fit curve of the experimental data meant the logarithmic number of the electron transfer rate constants of the mixed SAMs. The electron transfer rate constants of different redox densities and different modification methods were presented in Table-1.

The surface coverage, formal potentials and rate constants obtained for the redox monolayers, Fc-alkanethiolate and fc-capped-AuNPs modified surface, were presented in Table-1. It was observed that the rate constants had dependence on the surface coverage of ferrocenethiol for the same SAMs. In the present study, for the same SAMs, the electron transfer rate constant of the higher surface coverage of ferrocene was slower compared to that of the lower one, which might be attributed to the much lower

reorganization energy of the latter. It was clear that the lower percentage coverage of ferrocene would ensure reasonable isolation of the redox active sites in a bath of alkanethiol monolayer.

TABLE-1
CHARACTERISTICS OF THE MONOLAYERS

Components of SAMs	Γ (10^{-11} M/cm^2)	E^0, mM *vs.* Ag	k^0 (s^{-1})
FUT+MCH	1.52	544	3.5×10^3
	3.49	563	1.5×10^3
	35.10	571	6.3×10^2
FUT+MUH	0.12	536	6.1×10^3
	5.62	553	1.4×10^3
Fc-AuNP on MCH	4.08	578	1.2×10^2
Fc-AuNP on MUH	3.55	628	1.3

Γ = Surface coverage of ferrocene. E^0 = The oxidation potential of ferrocene in SAMs. k^0 = Standard rate constants were calculated following the method of Murray and coworkers as described in the text.

Comparison of FUT-MCH with Fc-AuNPs-MCH, both having the same bridge length, it revealed a much higher electron transfer rate (~10-fold) for the former at a similar coverage. It might be due to the orientation of gold nanoparticles had affected the electron transfer. This observation suggests that the contribution of the nanoparticles to the bridge-mediated electron transfer is greatly different from that of methylene groups. The Fc-AuNPs-MCH possessed a higher heterogeneous electron transfer rate constant than Fc-AuNPs-MCU although they had the similar coverage and the same orientation of the redox center. Under this conditions, the K_{ET} was only controlled by the bridge length between the redox molecules and the electrode, which was in agreement with that characteristic of a ferrocene in alkanethiol as reported[14].

It was well known that the colour of AuNPs solution was dependence on the distance among the particles which determined by electrostatic repulsion. A certain concentration of salt could change the colour of AuNPs by eliminating the repulsion. For the pure AuNPs, the colour of solution changed from red to blue in a few seconds when the concentration of NaCl reached 40 mM; as to the FUT-modified ones, the colour retained invariable for hours even if the final concentration of NaCl reached 100 mM. The results demonstrated that the ferrocenyl-undecanethiol had assembled on AuNPs and formed a compact monolayer which would stabilize the colloid. The stability quality of FUT had similar with thiolated single-strands DNA. Unlike the electronegative DNA, FUT is not electrical-loaded and the stability quality for AuNPs is probably due to the compact fabric formed by ferrocenethiol. It was presumed that the ferrocenethiol and thiolated DNA co-functionalized AuNPs would be applied to electrochemical biosensors as the electrochemical indicator.

ACKNOWLEDGEMENTS

The authors thank the financial support from National Natural Science Foundation (60537030 and 20404016), Shanghai Municipal Commission for Science and Technology (0652nm006 and 06ZR14106), Shanghai Rising-Star Program and Chinese Academy of Sciences.

REFERENCES

1. C. Joachim, J.K. Gimzewski and A. Aviram, *Nature*, **408**, 541 (2000).
2. S. Creager, C.J. Yu, C. Bamdad, S. O'Connor, T. MacLean, E. Lam, Y. Chong, G.T. Olsen, J.Y. Luo, M. Gozin and J.F. Kayyem, *J. Am. Chem. Soc.*, **121**, 1059 (1999).
3. K. Hu, Z. Chai, J.K. Whitesell and A.J. Bard, *Langmuir*, **15**, 3343 (1999).
4. H.X. Ju and D. Leech, *Langmuir*, **14**, 300 (1998).
5. H.X. Ju and D. Leech, *Phys. Chem. Chem. Phys.*, **1**, 1549 (1999).
6. T. Kondo, S. Horiuchi, I. Yagi, S. Ye and K. Uosaki, *J. Am. Chem. Soc.*, **121**, 391 (1999).
7. T. Kondo, T. Kanai, K. Iso-o and K. Uosaki, *Zeit. Phys. Chem. Int. J. Res. in Phys. Chem. & Chem. Phys.*, **212**, 23 (1999).
8. A.A. Kornyshev, A.M. Kuznetsov, J.U. Nielsen and J. Ulstrup, *Phys. Chem. Chem. Phys.*, **2**, 141 (2000).
9. A. Labande and D. Astruc, *Chem. Commun.*, 1007 (2000).
10. R.C. Sabapathy, S. Bhattacharyya, M.C. Leavy, W.E. Cleland and C.L. Hussey, *Langmuir*, **14**, 124 (1998).
11. Y. Sato, F. Mizutani, K. Shimazu, S. Ye and K. Uosaki, *J. Electroanal. Chem.*, **474**, 94 (1999).
12. K. Weber and S.E. Creager, *Anal. Chem.*, **66**, 3164 (1994).
13. S. Ye, T. Haba, Y. Sato, K. Shimazu and K. Uosaki, *Phys. Chem. Chem. Phys.*, **1**, 3653 (1999).
14. J.F. Smalley, H.O. Finklea, C.E. Chidsey, M.R. Linford, S.E. Creager, J.P. Ferraris, K. Chalfant, T. Zawodzinsk, S.W. Feldberg and M.D. Newton, *J. Am. Chem. Soc.*, **125**, 2004 (2003).
15. A.P. Alivisatos, *Science*, **271**, 933 (1996).
16. R.S. Ingram and R.W. Murray, *Langmuir*, **14**, 4115 (1998).
17. M.D. Musick, D.J. Pena, S.L. Botsko, T.M. McEvoy, J.N. Richardson and M.J. Natan, *Langmuir*, **15**, 844 (1999).
18. T. Nakanishi, B. Ohtani and K. Uosaki, *J. Electroanal. Chem.*, **455**, 229 (1998).
19. K.V. Sarathy, P.J. Thomas, G.U. Kulkarni and C.N.R. Rao, *J. Phys. Chem. B*, **103**, 399 (1999).
20. D. Goldhaber-Gordon, M.S. Montemerlo, J.C. Love, G.J. Opiteck and J.C. Ellenbogen, *Proc. of the IEEE*, **85**, 521 (1997).
21. C. Fan, K.W. Plaxco and A.J. Heeger, *Proc. Natl. Acad. Sci. USA*, **100**, 9134 (2003).
22. L. Tender, M.T. Carter and R.W. Murray, *Anal. Chem.*, **66**, 3173 (1994).
23. R.S. Nicholson and I. Shain, *Anal. Chem.*, **36**, 706 (1964).
24. E. Laviron, *J. Electroanal. Chem.*, **101**, 19 (1979).

(*Received*: 12 June 2007; *Accepted*: 1 December 2007) AJC-6104